

Impedance and Admittance Calculations of a Three-Core Power Cable by the Finite Element Method

Angelo. A. Hafner, Mauricio V. Ferreira da Luz, Walter P. Carpes Jr.

Abstract—The analytical modeling of a three-core cable system is challenging because of the non-concentric configuration of the components involved. Given these limitations, a 2D finite element modeling of the cable is developed in order to obtain the values of the self, mutual and sequence impedances and admittances. To calculate the series impedance, a magnetic vector potential magnetodynamic formulation is used and for the calculation of the parallel admittance, an electric scalar potential electrostatic formulation is applied. By calculating the series impedance of the inner cables, the influence of the mutual impedances in all metallic elements involved is shown. The methodology is applied to a typical cable of 300 mm² - 18/30 kV. The numerical results are compared with analytical ones and with values supplied by the manufacturer for each phase, validating the numerical modeling.

Keywords: Submarine power cable, 2D finite element method, impedance, admittance.¹

I. NOMENCLATURES

$I_0(\cdot)$	Bessel functions of first kind and order 0.
$I_1(\cdot)$	Bessel functions of first kind and order 1.
σ	Electric conductivity, in S/m.
ρ	Electric resistivity, in Ω m.
ε	Electric permittivity, in F/m.
μ	Magnetic permeability, in H/m.
ν	Magnetic reluctivity, in m/H.
SC	Semiconductor
\mathbf{M}	Matrix composed by matrixes.
\mathbf{m}	Matrix composed only by scalars.
\vec{V}, \vec{v}	Vector.
$(\cdot, \cdot)_{\Omega}$	Volume integral in Ω of products of scalar or vector fields.
$\langle \cdot, \cdot \rangle_{\Gamma}$	Surface integral on Γ of products of scalar or vector fields.
$\text{Im}(\cdot)$	Function that returns only the imaginary part of a complex number.
ω	Electrical angular frequency.
FEM	Finite Element Method.

Angelo A. Hafner is PhD student at the Department of Electrical Engineering, Federal University of Santa Catarina, Florianópolis, Brazil (e-mail: angelo.hafner@posgrad.ufsc.br)

Mauricio V. Ferreira da Luz is Professor at the Department of Electrical Engineering, Federal University of Santa Catarina, Florianópolis, Brazil (e-mail: mauricio.luz@ufsc.br)

Walter P. Carpes Jr is Professor at the Department of Electrical Engineering, Federal University of Santa Catarina, Florianópolis, Brazil (e-mail: walter.carpes@ufsc.br)

Paper submitted to the International Conference on Power Systems Transients (IPST2015) in Cavtat, Croatia June 15-18, 2015

II. INTRODUCTION

THE expansion of submarine transmission systems represents a major trend due to the growth of the oil and offshore wind energy industry. The deployment of these systems at large distances from the shore and in deep water requires kilometeric stretches of submarine power cables.

Fed equipment or systems, as well as cables, need to be adequately protected in case of short circuits, overloads and transients. An accurate cable model is needed to accurately represent the waveforms of voltage and current on the load and the transmission line providing technical support for the choice of the most suitable protection to be adopted for each situation.

When one considers the cable as single-core, the phases distributed impedances and admittances of the cable for a certain range of frequencies can be calculated analytically applying classical analytical formulae ((4), (6), and (11)). However, in three-core cables, even at 50/60 Hz, the following aspects should be taken into account when modeling: (i) proximity effect generated by the currents of the central conductor; and (ii) current induced in the sheath and its effects on the central conductor impedance [1].

The non-concentric configuration of the trefoil formation (Fig 1) hampers the analytical modeling. Thus, a 2D finite element model is developed to obtain the values of the cable series impedance and parallel admittance.

Some studies about cable modeling are presented in [1-6] and [16-22].

III. BASIC CHARACTERISTICS OF A SUBMARINE POWER CABLE

The physical constitution of submarine power cables is very similar to underground power cables.

The main difference is that in the first, there are additional protections for water entry (Fig. 1 and Table 1). In this section, we briefly describe the constituent parts of the submarine power cable as well as the aspects related to the calculation of its series impedance. Each part of the inner cable is described in Table 1. Small variations may occur from one manufacturer to another.

The cable of this study is composed of a set of three power inner cables in trefoil formation, as shown in Fig. 1. Parts 10-11, 11-12 and 12-13 consist of insulating material, conductor, and insulating, respectively. The conductive layer, called armor, has the main function of mechanically protecting the set.

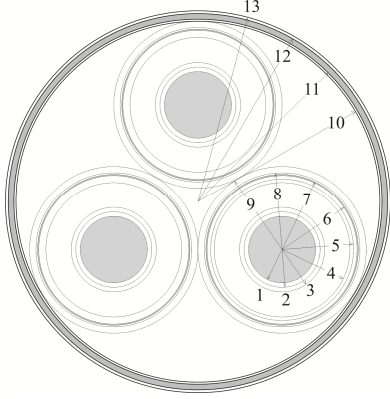


Fig. 1. Set of inner cables in trefoil formation of a three-core submarine power cable.

TABLE 1
PARTS OF A POWER INNER CABLE

Item	Component	Material
1	Core	Copper Stranded Wires
2	Water-blocking tape	Humidity absorber SC tape
3	Conductor Shield	SC tape
4	Insulation	XLPE
5	Insulation Shield	Humidity absorber SC tape
6	Water-blocking tape	Humidity absorber SC tape
7	Sheath	Copper wires
8	Water-blocking tape	Humidity absorber SC tape
9	Jacket	Polyethylene

IV. HOMOGENIZATION OF THE CORE

Because the materials are composed of several parts, homogenization techniques are applied to model them as solids used for both numerical and analytical approaches.

Homogenization in the core due to the natural gaps of the stranded conductor is made by the correction (increase) in resistivity since the core is now considered massive. This is done by applying:

$$\rho'_c = k_c \rho_c \quad (1)$$

where ρ'_c is the corrected resistivity of the central conductor, k_c is the area correction factor ($k_c = \pi r_c^2 / A_n$), r_c is the core radius, and A_n is the nominal area provided by the manufacturer's catalog.

Homogenization in sheath also depends on the composition of the material used. Therefore, its corrected resistivity is given by:

$$\rho'_s = k_s \rho_s \quad (2)$$

V. HOMOGENIZATION OF THE INSULATION

Between the core and insulation and sheath and insulation, there are semiconductor tapes which have the function of uniformly distributing the electric potential. These three materials are homogenized as one. For this, a correction must be applied to the insulation electric permittivity given by:

$$\varepsilon'_{cs} = \varepsilon_{cs} \frac{\ln(r_s/r_c)}{\ln(b/a)} \quad (3)$$

where ε_{cs} is the original insulation permittivity, and a and b are the inner and outer radii of the insulation, respectively.

VI. SERIES IMPEDANCE

The analytical modeling for non-concentric conductors, like the case of the three-core cables, is a very complex task. A full analytical computation of a submarine cable can be found using the pipe-type cable formulas from [3]. As explained in [4] there are some approximation in this, because of the representation of the armor.

Subsection *A* presents a way to calculate the phase impedance for a single-core cable, where only the impedance in a single inner cable can be considered without mutual couplings with any other metallic part of the cable. However, in the numerical approach, all couplings involved are regarded.

A. Analytical Approach

According to [3], [2], and [4], the impedance of each core per unit of length is given by:

$$z_c = \frac{\rho_c \xi_c}{2\pi r_c} \frac{I_0(\xi_c r_c)}{I_1(\xi_c r_c)}, \quad (4)$$

where ξ_c is the intrinsic medium impedance, given by:

$$\xi_c = \sqrt{j\omega\mu_c/\rho'_c}. \quad (5)$$

The core impedance z_c have one real part that represents the core resistance; and other part imaginary, that represents the internal core inductance times the electric angular pulsation.

The phase inductance is given by the sum of internal and external inductance. For a single core conductor, the external inductance is given by:

$$l_{ext_1C} = \frac{\mu_{cs}}{2\pi} \ln\left(\frac{r_c}{r_s}\right). \quad (6)$$

However (6) considers the current of central conductor returning by sheath. For three-core cables, the current returns by other phases, creating a bigger area for the magnetic flux, that now is the area between two phases. So (6) becomes:

$$l_{ext_3C} = \frac{\mu}{2\pi} \ln\left(\frac{r_c}{D}\right), \quad (7)$$

where D is the distance between cores in the trefoil formation. For other formations, the geometric mean must be applied.

Equation (7) is accurate and frequently used for impedance calculation at 50/60 Hz. For bigger frequencies, it is necessary to consider the sheath effects as covered by [5][6].

B. Numerical Approach

In order to find the self and mutual impedances of all metallic parts of the cable, a 1 A current is applied at one metallic element and measured the voltage in this and others. The self impedance is found by dividing the induced voltage by the current at the element that the current is applied. The mutual impedances are found by dividing the induced voltage at the elements that have no current by the current that

produced this induction.

C. Cable Impedances

Fig. 2 presents a three-core cable impedance diagram where: (i) the letters a , b , and c represent each core; (ii) the numbers 1, 2, and 3 represent each sheath; (iii) and g represents the armor.

The voltage drop from g to g' on conductors are:

$$\begin{bmatrix} V_{ag} - V_{a'g'} \\ V_{bg} - V_{b'g'} \\ V_{cg} - V_{c'g'} \\ V_{1g} - V_{1'g'} \\ V_{2g} - V_{2'g'} \\ V_{3g} - V_{3'g'} \\ V_g - V_{g'} \end{bmatrix} = \begin{bmatrix} z_{aa} & z_{ab} & z_{ac} & z_{a1} & z_{a2} & z_{a3} & z_{ag} \\ z_{ab} & z_{bb} & z_{bc} & z_{b1} & z_{b2} & z_{b3} & z_{bg} \\ z_{ac} & z_{bc} & z_{cc} & z_{c1} & z_{c2} & z_{c3} & z_{cg} \\ z_{a1} & z_{b1} & z_{c1} & z_{11} & z_{12} & z_{13} & z_{1g} \\ z_{a2} & z_{b2} & z_{c2} & z_{21} & z_{22} & z_{23} & z_{2g} \\ z_{a3} & z_{b3} & z_{c3} & z_{31} & z_{32} & z_{33} & z_{3g} \\ z_{ag} & z_{bg} & z_{cg} & z_{1g} & z_{2g} & z_{3g} & z_{gg} \end{bmatrix} \begin{bmatrix} I_a \\ I_b \\ I_c \\ I_1 \\ I_2 \\ I_3 \\ I_g \end{bmatrix} \quad (8)$$

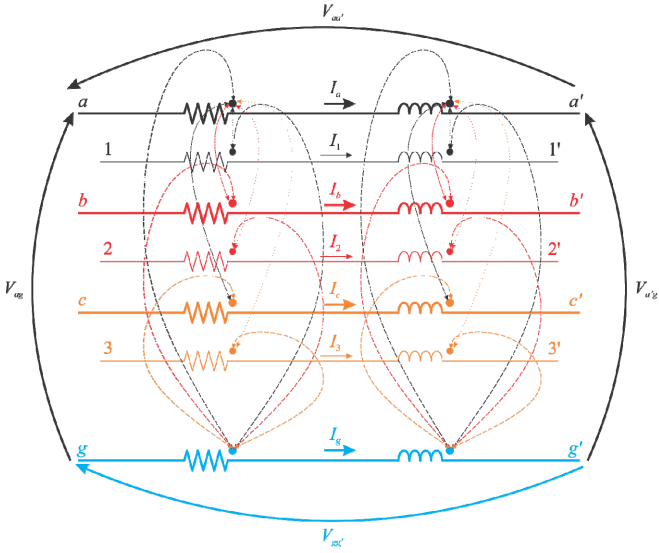


Fig. 2. Representation of three-core cable impedances.

In [5] it is proved that the sequence impedances for interconnected sheaths are:

$$z_+ = z_- = z_{aa} - z_{ab} - \frac{(z_{a1} - z_{a2})^2}{(z_{11} - z_{12})} \quad (9)$$

$$z_0 = z_{aa} + 2z_{ab} - \frac{z_{a1} + 2z_{a2}}{z_{11} + 2z_{a2}}$$

If the sheaths are not interconnected at both terminals, or are interconnected only at one point (grounded or not), there is not circulation current and the sequence impedances become [1]:

$$\begin{aligned} z_+ &= z_- = z_{aa} - z_{ab} \\ z_0 &= z_{aa} + 2z_{ab} \end{aligned} \quad (10)$$

VII. PARALLEL ADMITTANCE

There are three kinds of admittances on three-core cables: (i) core-sheath, (ii) sheath-sheath, and (iii) sheath-armor. Only the core-sheath armor is analytically feasible, given by:

$$y_{12} = \frac{2\pi(\sigma_{cs} + j\omega\varepsilon'_{cs})}{\ln(r_s/r_c)} \quad (11)$$

where σ_{cs} is the insulation conductivity and ε'_{cs} is the corrected permittivity of the insulation. Because of the high resistivity of the insulating materials, only the capacitances on them are considered (see Section VIII-B). The three-core cable capacitance diagram is shown in Fig. 3.

In addition, a numerical approach is performed and compared with the analytical results for this capacitance. However, for sheath-sheath and sheath-armor capacitances, only numerical results are considered due to the non-concentricity between these parts. The leakage currents on insulations from g to g' in phases are:

$$\begin{bmatrix} I_a - I_{a'} \\ I_b - I_{b'} \\ I_c - I_{c'} \\ I_1 - I_1 \\ I_2 - I_2 \\ I_3 - I_3 \end{bmatrix} = \begin{bmatrix} y_{cc} & 0 & 0 \\ 0 & y_{cc} & 0 \\ 0 & 0 & y_{cc} \end{bmatrix} \begin{bmatrix} y_{cs} & 0 & 0 \\ 0 & y_{cs} & 0 \\ 0 & 0 & y_{cs} \end{bmatrix} \begin{bmatrix} V_{ag} \\ V_{bg} \\ V_{cg} \end{bmatrix} \quad (12)$$

where y_{cc} , y_{cs} , y_{ss} and $y_{ss'}$ are, respectively, the core self-admittance, core-sheath mutual admittance, sheath self-admittance and sheath-sheath mutual admittance.

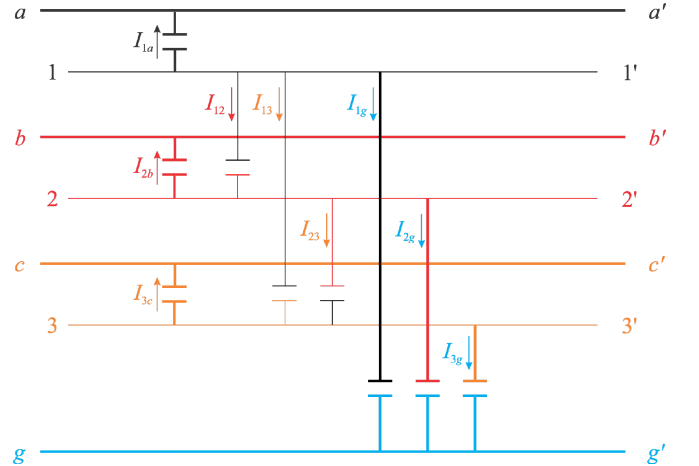


Fig. 3. The three-core cable capacitance diagram.

By using the technique presented in [7] it is possible to get:

$$y_{cc} = -y_{cs} = y_{a1}, \quad (13)$$

$$y_{ss} = y_{11} = y_{a1} + y_{1g} + y_{12} + y_{13} \quad (14)$$

$$y_{ss'} = -y_{12} = -y_{13} \quad (15)$$

VIII. NUMERICAL MODELING USING FEM

To perform the numerical modeling, the software Gmsh [8] and GetDP [9] are used. Gmsh is the pre and post-processor and the GetDP is the solver. The problem is implemented in the software by two codes: one that defines the geometries and the mesh of the structure (“geo” file) and other that defines the physical proprieties of the materials, the constraints and the formulation to be used (“pro” file).

The electrostatic formulation used to calculate of the

parallel admittance is given by:

$$(\varepsilon \text{grad} V, \text{grad} V')_{\Omega} + \langle \vec{n} \cdot \vec{D}, V' \rangle_{\Gamma_D} = (\rho_v, V')_{\Omega} \quad (16)$$

$$\forall V' \in F_v(\Omega)$$

where V is the electric scalar potential, V' is the test function for scalar potential, ρ_v is the volume charge density, \vec{n} is the unit normal vector exterior to Ω , and $\vec{n} \cdot \vec{D}$ is a constraint on the electric flux density associated with nonfixed potential boundaries Γ_D of the domain Ω , e.g. on floating potential boundaries Γ_f [14].

$F_v(\Omega)$ denotes the function space defined on Ω , which contains the basis and test functions for both scalar potentials V and V' [14]. At the discrete level, $F_v(\Omega)$ is approximated with nodal finite elements.

The harmonic magnetodynamic formulation used to calculate of the series impedance is given by:

$$(\nu \text{curl} \vec{A}, \text{curl} \vec{A}')_{\Omega} + \langle \vec{n} \times \vec{H}_s, \vec{A}' \rangle_{\Gamma_H} + (j\omega \vec{A}, \vec{A}')_{\Omega_c} + (\sigma \text{grad} V, \vec{A}')_{\Omega_c} - (\vec{J}_s, \vec{A}') = 0, \quad \forall \vec{A}' \in F_a(\Omega) \quad (17)$$

where σ is the electric conductivity defined on conducting parts Ω_c of Ω , \vec{A} is the magnetic vector potential, \vec{A}' is the test function for vector potential, \vec{J}_s is the source electric current density defined in Ω_s , and $\vec{n} \times \vec{H}_s$ is a constraint on the magnetic field associated with boundary Γ_H of the domain Ω [15]. $F_a(\Omega)$ denotes the function space defined on Ω which contains the basis and test functions for both vector potentials \vec{A} and \vec{A}' .

IX. METHODOLOGY

The physical and geometric data cable is obtained from manufacturer's catalog [10], for a three-core cable in trefoil formation.

Due to the complexity of the cable geometry, some simplifications like homogenization are required. In addition, it is imperative that some correction factors be applied before starting the simulation as explained in Section II.

A. Physical and geometry constants used in the model

At the central conductor, the copper resistivity is considered (17.24 nΩm). It is then corrected for a temperature of 90°C followed by an equivalent area (homogenization) resulting in a resistivity ρ'_c of 23.57 nΩm.

The transversal magnetic permeability used for all materials is considered μ_0 , even the armor, because it is composed of wires that are not in direct contact [11].

The cable is considered as totally surrounded by seawater with a conductivity of 5 S/m [12].

B. Simplified diagram of the cable

The parts considered for the cable model (analytic and numeric) are all solids and represented by Table 2 and Fig. 4.

C. The Finite Element Approach Implementation

Initially it is necessary to implement the surfaces (.geo file) from the model as shown in Table 2 and Fig. 4. In the same file, the mesh density factors must be inserted set in each point of the geometric figure.

Based on the geometry file, a mesh is built by Gmsh. Fig. 5(a) shows the mesh of the whole calculation domain while Fig. 5(b) shows the mesh of the lower left inner cable of the three-core cable, respectively, for the calculation of series impedance.

Both figures are shown with the aim of highlighting the mesh density utilized. Region A is a necessary region in order to avoid domain truncation errors, where the magnetic vector potential on its outer circle is zero. The physical constants values in this region are the same values as region B.

When calculating the parallel capacitance the electric scalar potential at the armor is set to zero.

TABLE 2

PARTS OF A POWER INNER CABLE

Item	Radius [mm]
1	10.20
2	20.60
3	20.72
4	24.00
5	51.75
6	53.75
7	57.95
8	61.95

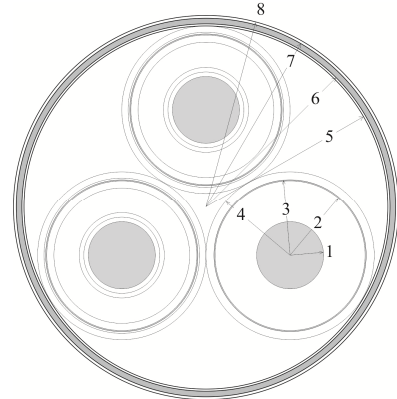


Fig. 4. Set of inner cables in trefoil formation of a three-core submarine power cable.

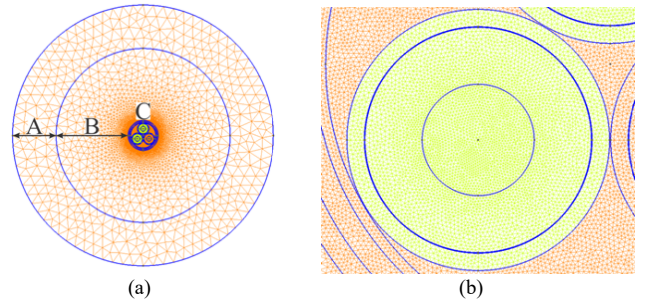


Fig. 5. Diagram and mesh for calculation of the series impedance. In (a) is the domain of calculation and in (b) the mesh detail of one power inner cable.

D. Obtaining the mutual and self-impedances and admittances

In order to find the self and mutual impedances of all metallic parts of the cable, the circuit presented in Fig. 6 is implemented and the technique explained in Section IV-B is applied.

The sequence impedances are also obtained where three short-circuited cores are fed by a 1 V / 50 Hz three-phase sinusoidal source (Fig. 7). For this implementation, two considerations are made: (i) with the sheath and armor opened; and (ii) with all sheaths interconnected at both ends and these connected to the respective armor end. The armor potential is considered floating (Fig. 7).

The representation of the diagrams shown in Fig. 6 and 7 illustrates as the electrical circuits are considered in GetDP. However, the modeling is carried out in two dimensions.

In order to find the parallel capacitance we apply the Maxwell Capacitance Matrix concept [7]. Firstly, a 1 V potential is applied on the core and zero on all other parts. The result is the core self-capacitance. After that it is applied a 1 V on the sheath and zero on all other parts (Fig. 8). From this measurement we find the sheath's self-capacitance which is the sum of sheath-core, sheath-sheath (2 times), and sheath-armor capacitances.

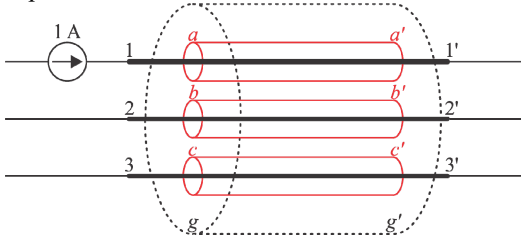


Fig. 6. Circuit diagram implemented in GetDP to determine the core self and mutual impedances.

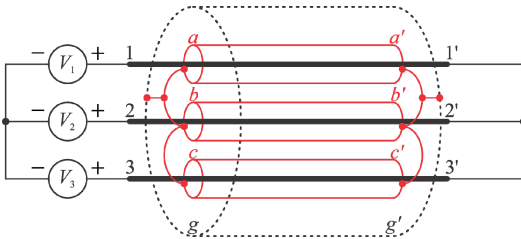


Fig. 7. Circuit diagram implemented in GetDP to determine the phase sequence impedances.

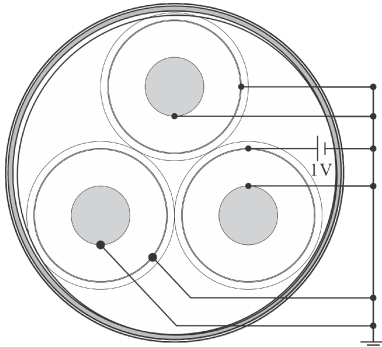


Fig. 8. Circuit diagram implemented in GetDP to determine the sheath self-capacitance.

To find the sheath 1-sheath 2 capacitance, is imperative, for instance, to apply 1 V to core *a*, sheath 1, core *c*, sheath 3, and armor, and zero on all other parts. The capacitance sheath 1-sheath 2 is obtained with basis on the electric flux that goes out from surface sheath 1. A similar procedure is applied to find core-sheath and sheath-armor capacitances.

Finally, the numerical results are compared with the analytical ones and also with the values supplied by the manufacturer for each phase, validating the numerical modeling.

X. RESULTS AND VALIDATION

The presentation of results is divided into two parts: (i) analysis of impedances, and (ii) analysis of admittances. Validations are made by comparison with analytical methods, when possible, and with manufacturer's catalog [10] for the frequency of 50 Hz.

A. Series impedance

At 50 Hz when we apply a current of $1 \angle 150^\circ$ A / 50 Hz to the core *a* (Fig. 9), we obtain the induced voltages shown in Table 3. Dividing the induced voltage in each metallic part of the cable by the current (imposed on core *a*) that originated them; we obtain the core self-impedance and the mutual impedance between the respective conductive part and the core (Table 4). Because it is a cable in trefoil formation (symmetric configuration), the same values are repeated when current is applied only in the core *b* or *c*.

TABLE 3
INDUCED VOLTAGE IN ALL CABLE CONDUCTIVE PARTS
WHEN CORE *a* IS FED BY $1 \angle 150^\circ$ A / 50 Hz

Voltage at:	Modulus [mV/km]	Angle [°]
Core <i>a</i>	414.1	-70.5
Core <i>b</i>	294.7	-60.0
Core <i>c</i>	294.7	-60.0
Sheath 1	347.2	-60.4
Sheath 2	294.7	-60.0
Sheath 3	294.7	-60.0
Armor <i>g</i>	285.2	-60.0

TABLE 4
CORE SELF-IMPEDANCE, MUTUAL BETWEEN CORES, MUTUAL CORE-SHEATH, AND MUTUAL CORE-ARMOR

Impedance	Resistance [mΩ/km]	Inductance [μH/km]
z_{aa}	75.7	1295.9
z_{ab}	0.0	938.1
z_{ac}	0.0	938.1
z_{a1}	2.4	1105.2
z_{a2}	0.0	938.1
z_{a3}	0.0	938.1
z_{ag}	0.0	907.9

One notices a great similarity in the values of mutual impedances between cores and between core and sheaths of other cores. In other words ($z_{ab} = z_{ac}$) \approx ($z_{a2} = z_{a3}$), as described

in Section 3.3 of [1].

The same process is repeated but now the current is applied to sheath 1 and the induced voltages in all the metallic elements of the cable are calculated. From this process Table 5 is formulated for sheath's self and mutual impedances. Finally, the calculation is repeated applying current at the armor and calculating the other induced voltages, resulting in Table 6.

As expected, independent of where the current is applied, the mutual impedances are always the same as evidenced in Tables 4, 5, and 6.

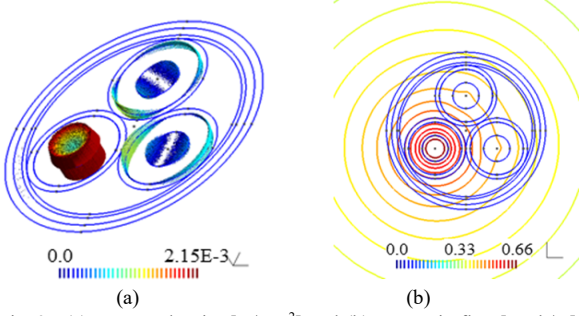


Fig. 9. (a) Current density [A/mm²] and (b) Magnetic flux [μWb/m] used for the calculation of core self and mutual sequence impedances via FEM.

TABLE 5
CORE-SHEATH MUTUAL IMPEDANCE, SHEATH SELF,
AND MUTUAL SHEATH-ARMOR

Impedance	Resistance [mΩ/km]	Inductance [μH/km]
z_{1a}	2.4	1105.2
z_{1b}	0.0	938.1
z_{1c}	0.0	938.1
z_{11}	1731.3	1104.9
z_{12}	0.0	938.1
z_{13}	0.0	938.1
z_{1g}	0.0	907.9

TABLE 6
CORE-ARMOR MUTUAL, SHEATH-ARMOR MUTUAL,
AND ARMOR SELF-IMPEDANCE

Impedance	Resistance [mΩ/km]	Inductance [μH/km]
z_{ga}	0.00	907.9
z_{gb}	0.00	907.9
z_{gc}	0.00	907.9
z_{g1}	0.00	907.9
z_{g2}	0.00	907.9
z_{g3}	0.00	907.9
z_{gg}	616.8	905.4

If the sheaths are interconnected only at one of the ends (whether grounded or not), only the mutual impedances between cores influence the phase positive sequence impedance, which for the inductance can be obtained from (10):

$$L_+ = 1295.9 - 938.1 = 0.3578 \text{ mH/km} \quad (18)$$

The series inductance value of the cable in the manufacturer's catalog [10] is 0.36 mH/km, which validates the accuracy of the method used.

Similarly we obtain the value of the positive sequence resistance:

$$R_+ = 75.7 - 0.0 = 75.7 \text{ mΩ/km} \quad (19)$$

The positive sequence impedance are also determined when three balanced voltages are applied, displaced 120 degrees from each other, with the three cores short-circuited and the sheaths and armor opened (Fig. 10). Values equal to those found in (18) and (19) are obtained.

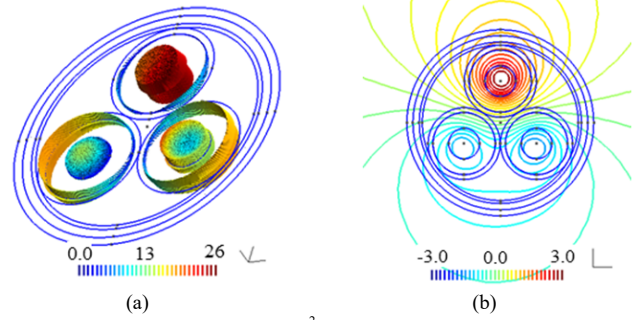


Fig. 10. (a) Current density [A/mm²] and (b) Magnetic Flux [mWb/m] used for the calculation of positive sequence impedance directly via FEM.

Finally, an analytical approach is made by applying of (4) and (7).

Table 7 presents a comparison of the results obtained for the positive sequence resistance and inductance between the adopted approaches. The error is found by taking the reference value provided by the manufacturer. The manufacturer did not provide the distributed cable resistance value.

If the sheaths are connected at both ends, the distributed positive sequence series resistance and inductance would be: $R_+ = 77.3 \text{ mΩ/km}$ and $L_+ = 357.83 \text{ μH/km}$.

TABLE 7
INDUCTANCE PROVIDED BY THE MANUFACTURER, CALCULATED
ANALYTICALLY, AND CALCULATED VIA FEM

	R_+ [mΩ/km]	L_+ [mH/km]	L_+ Error [%]
Manufacturer	---	0.360	---
Analytical	73.2	0.359	0.171
Numeric	77.3	0.358	0.603

The increase in resistance occurs because, when the sheaths are interconnected, a circulation path is created for the induced currents. The introduction of an effect in the core current distribution is therefore due to the sheath's current increasing the proximity effect in the respective core compared to the case where the sheaths are not interconnected. As the frequency increases, this effect is increased [13].

Knowing the resistances and inductances (selves and mutual) found for all conductive parts of the cable, the impedance matrix can be mounted:

$$\mathbf{Z} = \begin{bmatrix} \mathbf{z}_{core} & \mathbf{z}_{core-sheath} & \mathbf{z}_{core-armor} \\ \mathbf{z}_{core-sheath} & \mathbf{z}_{sheath} & \mathbf{z}_{sheath-armor} \\ \mathbf{z}_{core-armor} & \mathbf{z}_{sheath-armor} & \mathbf{z}_{armor} \end{bmatrix} \quad (20)$$

where, \mathbf{z}_{core} , \mathbf{z}_{sheath} , $\mathbf{z}_{core-sheath}$, \mathbf{z}_{armor} , $\mathbf{z}_{core-armor}$, $\mathbf{z}_{sheath-armor}$, are, in $\mu\Omega/m$:

$$\mathbf{z}_{core} = \begin{bmatrix} 75.7 + j407 & j295 & j295 \\ j295 & 75.7 + j407 & j295 \\ j295 & j295 & 75.7 + j407 \end{bmatrix} \quad (21)$$

$$\mathbf{z}_{sheath} = \begin{bmatrix} 1731 + j347 & j295 & j295 \\ j295 & 1731 + j347 & j295 \\ j295 & j295 & 1731 + j347 \end{bmatrix} \quad (22)$$

$$\mathbf{z}_{core-sheath} = \begin{bmatrix} 2.39 + j347 & j295 & j295 \\ j295 & 2.39 + j347 & j295 \\ j295 & j295 & 2.39 + j347 \end{bmatrix} \quad (23)$$

$$z_{armor} = 616 + j285$$

$$z_{core-armor} = j295 \quad (24)$$

$$z_{sheath-armor} = j295$$

B. Parallel admittance

Because the insulating material has a high resistivity, the branch that represents the parallel conductance can be neglected, which can be seen already at 50 Hz by applying (11) to the cable under consideration (XLPE insulation), where $a = 11.4$ mm and $b = 19.4$ mm.

$$y_{12} = (0.0098 + j82.184) \text{ nS/m} \quad (25)$$

The core-sheath capacitance is $\text{Im}(y_{12})/\omega = 261.60$ pF/m, very close to the value provided by the manufacturer's catalog [10], which is 0.26 $\mu\text{F}/\text{km}$.

The core-sheath capacitance is also calculated through finite element technique, obtaining the value of 261.60 pF/m, which is exactly the value found by the analytical method (also very close to the value provided by the manufacturer). Fig. 11 shows the electric field in the region under analysis (as well as in sheath-sheath and sheath-armor regions).

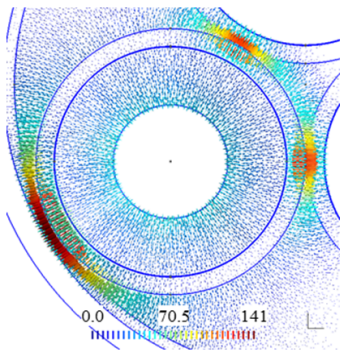


Fig. 11. Electric field [V/m] lines when a 1 V potential is applied at the sheath 1 and 0 V to all other metallic parts of the cable, to obtain the sheath self-capacitance.

Finally, the capacitance sheath-sheath and sheath-armor by the finite element method are calculated. Table 8 shows the cables' capacitances values between core and sheath, sheath and sheath and sheath and armor, as also the error of measurement, considering the value of the manufacturer [10] as reference.

According to (12), the parallel capacitance matrix is:

$$\mathbf{Y} = j\omega\mathbf{C}, \quad (26)$$

where \mathbf{C} , in pF/m, is:

$$\mathbf{C} = \begin{bmatrix} 262 & 0 & 0 & -262 & 0 & 0 \\ 0 & 262 & 0 & 0 & -262 & 0 \\ 0 & 0 & 262 & 0 & 0 & -262 \\ -262 & 0 & 0 & 510 & 54.4 & 54.4 \\ 0 & -262 & 0 & 54.4 & 510 & 54.4 \\ 0 & 0 & -262 & 54.4 & 54.4 & 510 \end{bmatrix} \quad (27)$$

TABLE 8

CAPACITANCE OF THE THREE-CORE CABLE IN STUDY

Region	Numeric [$\mu\text{F}/\text{km}$]	Analytical [$\mu\text{F}/\text{km}$]	Manuf. [$\mu\text{F}/\text{km}$]	Error [%]
Core-Sheath	0.2616	0.2616	0.26	0.006
Sheath-Sheath	0.0544	---	---	---
Sheath-Armor	0.1401	---	---	---

XI. CONCLUSIONS

Space in manufacturer's cable catalogs is typically dedicated only for distributed positive sequence inductance and capacitance values at industrial frequency (50 or 60 Hz). In [13] it is presented for the same cable of present study, the behavior of positive sequence impedances for a frequency range from 20 Hz to 20 kHz.

In the present work, it was considered 50 Hz, with the improvement to find the parallel admittance and the specificity in relation to mutual coupling between phases, thereby allowing to get the sequence impedances.

Similar to what was done in reference [13], in future works the goal will be to evolve the work presented in this paper by examining the frequency range from 20 Hz to 20 kHz. We will intend: (i) to simulate underground cables with grounded ends; and (ii) to apply the same modeling of this paper without the application of homogenization techniques (such as those applied in the central conductor and sheath in Section III). It is expected that through this study, an increase in the accuracy of the model's response, especially at high frequencies, may be achieved. Moreover, field measurements have to be made for validation.

XII. ACKNOWLEDGEMENT

The authors would like to gratefully acknowledge the PETROBRAS for the financial support to this research effort.

XIII. REFERENCES

- [1] F. F. Da Silva and C. L. Bak, *Electromagnetic Transients in Power Cables*. Springer London, Limited, 2013.
- [2] S. A. Schelkunoff, "The Electromagnetic Theory of Coaxial Transmission Lines and Cylindrical Shields," *Bell Syst. Tech. J.*, p. 47, 1934.
- [3] A. Ametani, "A General Formulation of Impedance and Admittance of Cables," *IEEE Trans. Power Appar. Syst.*, vol. PAS-99, no. 3, pp. 902-910, May 1980.

- [4] A. Pagetti, "Cable Modeling for Electromagnetic Transients in Power Systems," Université Blaise Pascal - Clermont II, 2012.
- [5] T. Aloui, F. Ben Amar, and H. H. Abdallah, "Modeling of a three-phase underground power cable using the distributed parameters approach," in *Systems, Signals and Devices (SSD), 2011 8th International Multi-Conference on*, 2011, pp. 1–6.
- [6] W. A. Lewis and G. D. Allen, "Symmetrical-Component Circuit Constants and Neutral Circulating Currents for Concentric-Neutral Underground Distribution Cables," *Power Appar. Syst. IEEE Trans.*, vol. PAS-97, no. 1, pp. 191–199, Jan. 1978.
- [7] E. Di Lorenzo, "The Maxwell Capacitance Matrix," no. March, pp. 1–3, 2011.
- [8] C. Geuzaine and J.-F. Remacle, "Gmsh Reference Manual." 2013.
- [9] P. Dular and C. Geuzaine, "GetDP Reference Manual." 2013.
- [10] ABB, "XLPE Submarine Cable Systems." Available at (15/april/2015): [http://www04.abb.com/global/seitp/seitp202.nsf/0/badf833d6cb8d46dc1257c0b002b3702/\\$file/XLPE+Submarine+Cable+Systems+2GM5007+.pdf](http://www04.abb.com/global/seitp/seitp202.nsf/0/badf833d6cb8d46dc1257c0b002b3702/$file/XLPE+Submarine+Cable+Systems+2GM5007+.pdf).
- [11] "IEC 287-1-1: 'Electric cables-calculation of the current rating, part 1: current rating equations (100% load factor) and calculation of losses, section 1: general.'" 1994.
- [12] L. Rossi and J.-P. Thibault, "Investigation of wall normal electromagnetic actuator for seawater flow control," *J. Turbul.*, Aug. 2007.
- [13] A. A. Hafner, M. V. F. da Luz, F. F. da Silva, W. P. Carpes Jr., and S. de Lima, "Aplicação do Método de Elementos Finitos no Cálculo da Impedância Distribuída em Cabos de Potência Tripolares," in *16 SBMO - Simpósio Brasileiro de Micro-ondas e Optoeletrônica e 11 CBMag - Congresso Brasileiro de Eletromagnetismo (MOMAG 2014), 2014 (in Portuguese)*.
- [14] P. Dular, W. Legros, and A. Nicolet, "Coupling of local and global quantities in various finite element formulations and its application to electrostatics, magnetostatics and magnetodynamics," *IEEE Transactions on Magnetics*, vol. 34, no. 5, pp. 3078–3081, September 1998.
- [15] M. V. Ferreira da Luz, "Desenvolvimento de um software para cálculo de campos eletromagnéticos 3D utilizando elementos de aresta, levando em conta o movimento e o circuito de alimentação", PhD Thesis (in Portuguese), Federal University of Santa Catarina, Brazil, 2003.
- [16] Multiwire shielded cable parameter computation. Kane, M.; Ahmad, A.; Auriol, P. *IEEE Transactions on Magnetics*. Volume: 31, Issue: 3. Publication Year: 1995, Page(s): 1646-1649.
- [17] Yin, Y.; Dommel, H.W. Calculation of frequency-dependent impedances of underground power cables with finite element method. *IEEE Transactions on Magnetics*. Volume: 25, Issue: 4. Publication Year: 1989, Page(s): 3025-3027
- [18] Xiao-Bang Xu; Guanghao Liu; Chow, P. A finite-element method solution of the zero-sequence impedance of underground pipe-type cable. *IEEE Transactions on Power Delivery*. Volume: 17, Issue: 1. Publication Year: 2002, Page(s): 13-17
- [19] Andreou, G.T.; Labridis, D.P. Electrical Parameters of Low-Voltage Power Distribution Cables Used for Power-Line Communications. *IEEE Transactions on Power Delivery*. Volume: 22, Issue: 2. Publication Year: 2007, Page(s): 879-886.
- [20] Gustavsen, B.; Bruaset, A.; Bremnes, J.J.; Hassel, A. A Finite-Element Approach for Calculating Electrical Parameters of Umbilical Cables. *IEEE Transactions on Power Delivery*. Volume: 24, Issue: 4. Publication Year: 2009, Page(s): 2375-2384.
- [21] Hoidalen, H.K. Analysis of Pipe-Type Cable Impedance Formulations at Low Frequencies. *IEEE Transactions on Power Delivery*. Volume: 28, Issue: 4. Publication Year: 2013, Page(s): 2419-2427.
- [22] de Arizon, Paloma; Dommel, H.W. Computation of Cable Impedances Based on Subdivision of Conductors. *IEEE Transactions on Power Delivery*. Volume: 2, Issue: 1. Publication Year: 1987, Page(s): 21-27.